Preprints.org

Article

Changing Law of Permeability of Coal Reservoirs under Variable Pressure Conditions and Its Influence on Extraction Efficiency of Coalbed Methane

Jianbao Liu , Zhimin Song , Chengtao Yang [*] , Bing Li , Jiangang Ren , Shengjie Chen

Article

Changing Law of Permeability of Coal Reservoirs under Variable Pressure Conditions and Its Influence on Extraction Efficiency of Coalbed Methane

Jianbao Liu [1,2], Zhimin Song [1,2,3], Chengtao Yang [4,*], Bing Li [1], Jiangang Ren [1] and Shengjie Chen [1]

[1] Henan University of Engineering, Zhengzhou 451191, China
[2] Henan Polytechnic University, Jiaozuo 454000, China
[3] North China University of Water Resources and Electric Power, Zhengzhou 450046, China
[4] Henan energy and Chemical Industry Group Research Institute Co., Ltd, Zhengzhou 450046, China
* Correspondence: byctat@163.com

Abstract: Coal permeability data are critical in the prevention and control of coal and gas outbursts in mines and are an important reservoir parameter for the development of coalbed methane. The mechanism by which permeability is affected by gas pressure is complex. We used a self-developed true triaxial seepage experimental device that collects lignite and anthracite coal samples, sets fixed axial pressure and confining pressure, and changes gas pressure by changing the orientation of the coal seam to study the influence of the gas pressure on the permeability of the coal seam under the conditions of different coal types and different bedding orientations. Coal permeability decreased rapidly and then decreased slowly and tended to be stable with the increase in gas pressure. This conforms to the power exponential fitting relationship, and the fitting degree reaches more than 99%. The permeabilities of lignite and anthracite were basically the same under various pressure conditions, indicating that the influence of coal type on coal permeability was not significant. The comparison of the two anthracite coal samples showed that the sample's permeability with a bedding plane vertical to the seepage direction was significantly lower than that of the bedding plane parallel to the seepage direction, indicating that gas seeped more easily along the bedding. The sensitivity coefficient of permeability with the change in gas pressure was calculated. The analysis showed that coal permeability was sensitive to changes in gas pressure during the low-pressure stage. When the gas pressure was greater than 0.8 MPa, the sensitivity coefficient was significantly reduced, which may be related to the slow increase in the amount of gas absorbed by the coal seam in the high-pressure stage. A theoretical calculation model of coal seam permeability considering adsorption/desorption and seepage effects was proposed and then verified with experimental results showing that the theoretical model better reflected the permeability characteristics of coal and predicted its permeability. Using the finite element simulation software COMSOL, the extraction efficiency of the coal seam gas under different gas pressure conditions was simulated. The results showed that with an increase in gas pressure, coal permeability and extraction efficiency decreased. In the low-pressure stage, the reduction in the extraction efficiency was more obvious than that in the high-pressure stage.

Keywords: true triaxial seepage experiment; gas pressure; metamorphic degree; bedding direction; permeability; extraction efficiency

1. Introduction

China is rich in coalbed gas. As an unconventional natural gas resource, gas has substantial potential and value for exploitation. However, gas is a main factor in coal and gas outbursts, and its greenhouse effect is 22 times greater than that of CO_2. Coal seam gas extraction effectively reduces gas emissions from coal mines and coal and gas outburst accidents. Coal permeability is an important parameter that affects the flow of coalbed gas and the efficiency of coalbed gas extraction. Many relevant experiments and theoretical and numerical simulations regarding the factors influencing coal permeability have reached important conclusions [1–5].

In coalbed gas extraction, coal permeability is affected by effective stress, gas pressure, gas adsorption/desorption characteristics, pore and fissure structure characteristics, and slippage effects

[6,7]. Regarding the relationship between gas pressure and coal permeability, the main understandings in the literature are as follows: First, coal permeability decreases and then increases with the decrease in gas pressure, the critical gas pressure of the inflection point of coal permeability in different basins differs, and gas pressure and permeability have a quadratic polynomial fitting relationship. Second, the slippage effect has an obvious influence on coal permeability at the low-pressure stage, and the slippage effect is related to the shape and size of fractures [8,9]. During the process of coalbed methane development or gas extraction, with the continuous production of gas, the gas pressure in the coal reservoir gradually decreases, resulting in dynamic changes in its permeability and affecting extraction efficiency. Therefore, studying the dynamic law of coal permeability during gas pressure changes is critical. The coal body exists in a three-dimensional stress state. During coal mining disturbances, the influence of changes in stress and gas pressure on the fracture and permeability of the coal body cannot be ignored. Therefore, in studying the influence of gas pressure on coal permeability, the in situ stress state of coal in the ground should be reduced as much as possible.

In this paper, the change in coal seam permeability with gas pressure was assessed using a self-developed true triaxial stress-seepage test device under a fixed axial and confining pressure. Next, a theoretical analysis and a comparison with experimental data were conducted, and a mathematical model of the permeability change with air pressure was proposed. Finally, the influence of gas pressure on gas extraction efficiency was calculated using COMSOL.

2. Materials and Methods

The samples for the experiments were collected from the Lu'an mining area in Shanxi Province, China. Whole coal samples were collected from the working face, crushed, placed on plastic sheets, and sent to the laboratory. The coal samples were cut and ground into cubic test pieces, each 100 × 100 × 100 mm. Three coal samples were used in the test: one lignite and two anthracite coal samples labeled HM, WY[1], and WY[2], respectively. Specifically, HM represents the lignite coal sample in which the bedding layer is parallel to the gas seepage direction, WY[1] represents the anthracite coal sample in which the bedding layer is parallel to the gas seepage direction, and WY[2] represents the anthracite coal sample in which the bedding layer is perpendicular to the gas seepage direction (the same below). The industrial analysis and R_o max values of the coal samples are listed in Table 1. The maximum vitrinite reflectances of the coal samples were 0.5, 2.6, and 2.5.

Table 1. Industrial analysis and R_o max of the coal samples

Coal types	Industrial analysis				R_o max(%)
	M_{ad}/%	A_d/%	V_{daf}/%	FC_{ad}/%	
HM	10.23	35.62	25.65	35.48	0.5
WY[1]	2.36	15.58	9.03	76.24	2.6
WY[2]	2.43	16.67	8.75	77.45	2.5

Note: M_{ad} is moisture on an air-dried basis, A_d is ash on a dry basis, V_{daf} is volatile matter on a dry ash-free basis, and FC_{ad} is carbon on an air-dry basis; R_o max is the maximum reflectance.
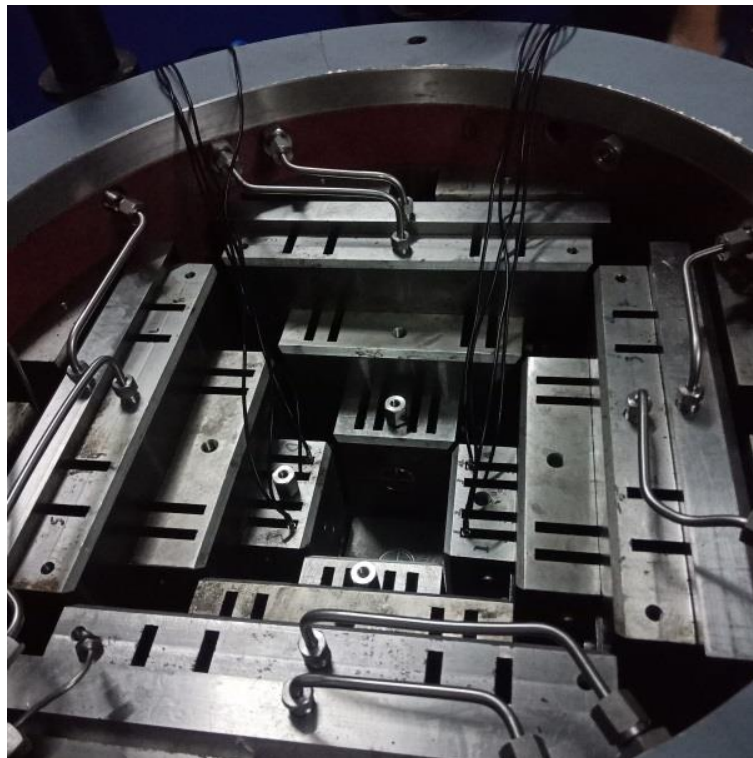
Our research group independently designed and developed the true triaxial stress-permeability test device used in this experiment (Figs. 1 and 2). The experimental equipment simulates the change law of the coal reservoir permeability in a true triaxial stress environment by adjusting parameters, for example, the horizontal crustal stress, vertical crustal stress, gas pressure, gas type, and temperature. The experimental results provide a reference for the prevention and control of coal and gas outbursts in coal mines, as well as technical support for the exploration and development of coalbed methane. The device was able to adopt three coal sample sizes: 300 mm × 300 mm × 300 mm, 200 mm × 200 mm × 200 mm, and 100 × 100 × 100 mm and 100 × 100 × 100 mm. This study used 100 mm × 100 mm × 100 mm coal samples. The maximum confining pressure was 40 MPa, and the accuracy was ± 0.1 MPa. The measurement range of gas permeability was 0.001 mD 1000 mD.

In the literature, coal samples were sealed with silica to prevent gas leakage along their edges during the seepage tests [10]. However, when the axial or confining pressure reaches a certain level,

the silicone sleeve is mostly cut off. Therefore, the development of new sealing materials for this purpose has been ongoing. Copper exhibits good strength and ductility. Under large confining or axial pressures, it can effectively seal coal samples without crushing them, satisfying the experimental requirements. Therefore, this study used a copper-rubber sleeve to seal the coal samples in the seepage test.

Figure 1. Overall layout of true triaxial permeability tester.
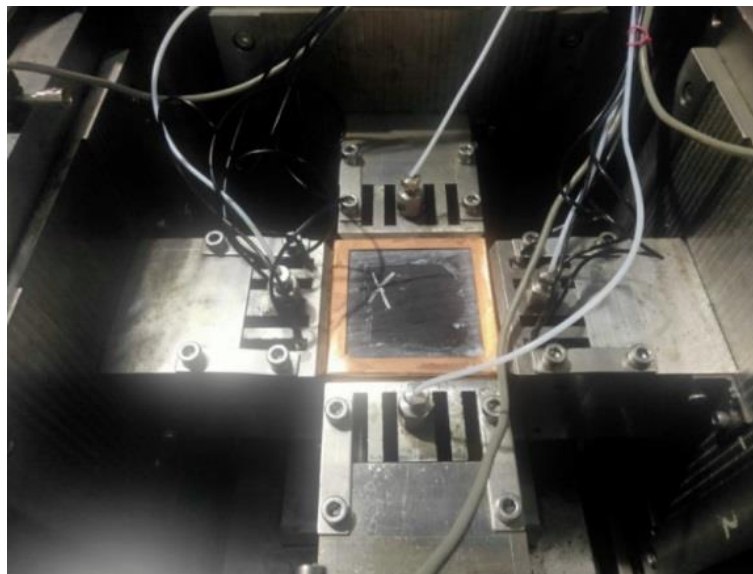

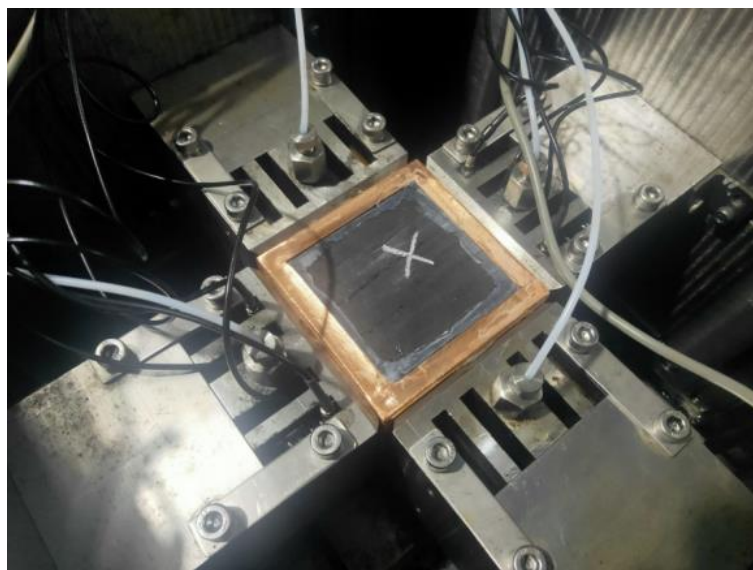**Figure 2.** Sample holder of true triaxial permeability tester.

The prepared coal samples were placed in a triaxial pressure chamber according to the operating instructions of the experimental device, and various auxiliary equipment was installed. The axial and confining pressures were synchronously loaded to a preset value of 15 MPa by using force control. Next, 0.5 MPa CH_4 was added via the air inlet, and the state was unchanged until adsorption equilibrium was reached. The adsorption equilibrium time was determined based on the experimental adsorption and desorption data. The axial pressure and confining pressure were maintained such that they were unchanged. Subsequently, the gas pressure was loaded one by one in the order of 0.5, 1.0, and 1.5 MPa by adjusting the gas pressure valve. The corresponding data were recorded after each gas pressure point reached the desorption balance and the flow was stable.

To study the influence of coal quality and bedding orientation on coal permeability, during this experiment, the lignite coal sample HM and the anthracite coal sample WY[1] were placed vertically, and the vertical bedding plane was parallel to the inlet seepage direction of CH_4 (Figs. 3 and 4). The anthracite coal sample WY[2] was placed vertically, and the vertical layer was perpendicular to the inlet seepage direction of CH_4 (Fig. 5) for comparison with the anthracite coal sample WY[1] and to study the influence of bedding orientation on coal permeability.

Figure 3. HM bedding plane is parallel to gas inlet direction.

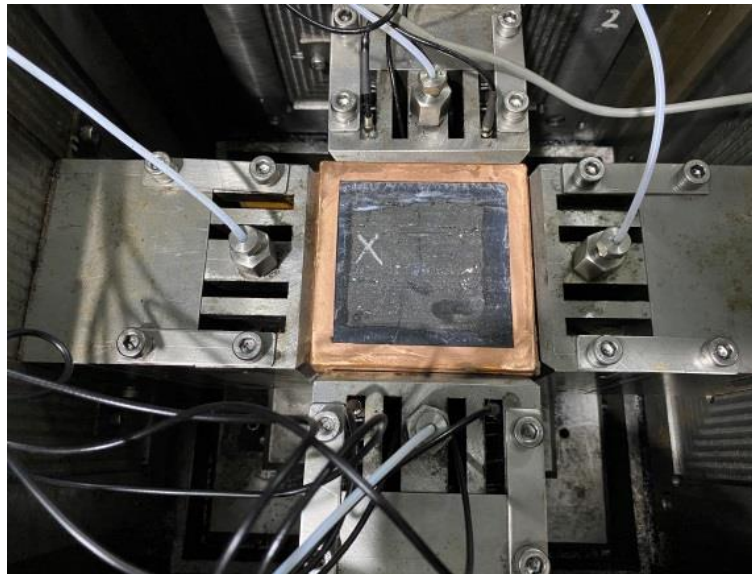**Figure 4.** WY[1] bedding plane is parallel to gas inlet direction.

Figure 5. WY² bedding plane is perpendicular to gas inlet direction.

3. Results

As shown in Figure 6, when the axial and confining pressures were constant, the permeability of the coal decreased gradually with an increase in the pore pressure. When the pore pressure increased from 0.5 to 0.8 MPa, coal permeability decreased rapidly. When the pore pressure increased from 0.8 to 1.5 MPa, coal permeability decreased slowly. Possible reasons for these findings are as follows: ① With the increase in gas pressure, the effective stress of the coal body decreased, and the opening of coal body cracks increased, increasing permeability; ② The adsorption and expansion deformation of the coal matrix increased with the increase in gas pressure, squeezing the fracture and reducing fracture width and coal permeability; ③ In the low-pressure region below 0.8 MPa, the slippage effect was significant, and the slippage effect gradually decreased with the increase in pore pressure [11–15]. The change trend of permeability with an increase in gas pressure demonstrates that in the range of experimental gas pressures, the expansion deformation caused by the adsorption of gas on the coal matrix plays a leading role, and the inhibition effect of adsorption expansion on permeability is always greater than the beneficial effect of effective stress reduction on permeability growth. When the pore pressure reached a certain value, the adsorption amount gradually reached saturation, and the reduction trend of the permeability became flat. In addition, with the weakening of the slippage effect, the permeability trend sharply decreased and then gradually decreased with the increase in pore pressure.
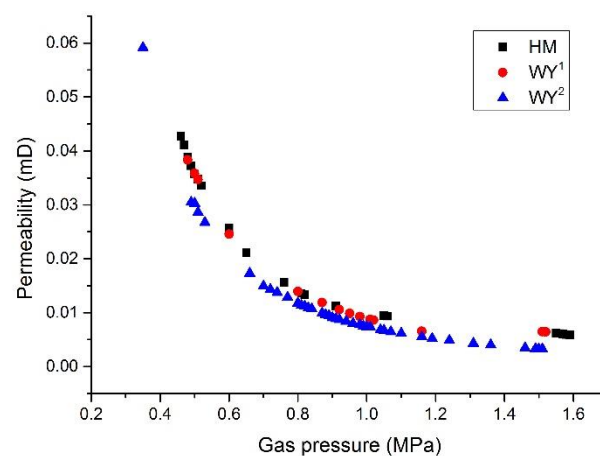

Figure 6. Change law of permeability with gas pressure.

4. Discussion

4.1. Gas pressure sensitivity analysis

In the quantitative exploration of the response of permeability to gas pressure, the relative change in coal permeability caused by each reduction in unit gas pressure under constant stress was defined as the sensitivity coefficient of permeability to gas pressure C_p:

$$C_p = -\frac{1}{k_0}\frac{\partial k}{\partial p}, \tag{1}$$

where C_p is the gas pressure sensitivity coefficient, mPa^{-1}; ∂k is the permeability change in coal, μ m^2; ∂p is the change in gas pressure, mPa; and k_0 is the initial permeability value, indicating coal permeability when the gas pressure is 0.5 mPa.

Figure 7 shows the gas pressure sensitivity coefficient of coal sample permeability under the experimental conditions of this study. The sensitivity coefficient and gas pressure data were fitted in accordance with a power function relationship, and the degree of fit was above 90% (Table 2). The sensitivity coefficient C_p decreased with an increase in gas pressure, decreased faster before 0.8 mPa, and tended to be stable after 0.8 mPa. According to the relationship between desorption amount and gas pressure, when gas pressure is low, the increment of CH$_4$ adsorption by coal particles is large [16–19]. In addition, the slippage effect is more pronounced in the low-pressure region. Therefore, the sensitivity coefficient C_p of the permeability to the gas pressure in the low-pressure zone was relatively large. When the gas pressure was high, the increase in CH$_4$ adsorption by the coal particles tended to be stable, and the effect of matrix expansion on permeability was small. Therefore, C_p is small in the high-pressure area. Also shown in Figure 7 is that the sensitivity coefficient of the bedding plane perpendicular to the seepage direction was less than that of the bedding plane parallel to the seepage direction.
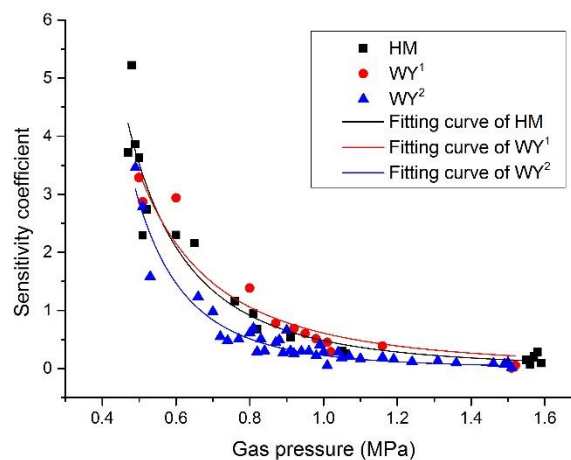

Figure 7. Relation curve between sensitivity coefficient and gas pressure.

Table 2. Fitting of sensitivity coefficient of coal permeability

Coal sample	Fitting equation	Fit R^2
HM	$C_p = 0.48095p^{-2.87622}$	0.91913
WY^1	$C_p = 0.60954p^{-2.47003}$	0.92759
WY^2	$C_p = 0.22574p^{-3.66777}$	0.93473

4.2. Mathematical model of coal permeability

4.2.1. Mathematical model

According to the literature, the volume deformation of coal owing to desorption or adsorption has a linear relationship with the amount of gas adsorption [20–22]:

$$\varepsilon_V = \varepsilon \times V, \tag{2}$$

where ε_V is the deformation of gas adsorption or desorption; ε is the volumetric strain coefficient, taking the value of 7.4×10^{-4} g/cm³; and V is the adsorption amount of gas. The gas adsorption capacity V can be obtained from the Langmuir adsorption curve [23–25]:

$$V = \frac{V_L p}{p + p_L},$$

(3)

where V and V_L denote the gas adsorption capacities at pressures p and p_L, respectively.

Chikatamarl's gas adsorption test shows that the volume strain of coal caused by gas adsorption is proportional to the amount of gas adsorbed. According to rock mechanics, the stress and strain of the deformation of the coal body absorbing gas can be expressed as [26–29]

$$\sigma_{i,j} = \frac{E}{1+v}\left(\varepsilon_{i,j} + \frac{v}{1-2v}\varepsilon_b \delta_{i,j}\right) + \alpha p \delta_{i,j} + K\varepsilon_V \delta_{i,j},$$

(4)

where ε_V is the deformation of gas adsorption or desorption, which can be obtained from formula (2); E is Young's modulus; v is Poisson's ratio; K is the bulk modulus of elasticity, with $\alpha = 1 - K/K_s$, K_s being the modulus of the solid matrix. The bulk modulus K is often several orders of magnitude larger than the pore bulk modulus K_p of coal, where $\delta_{i,j}$, the Kronecker delta, is zero when $i \neq j$ and one when $i = j$, and the Einstein summation convention is followed. The available permeability is [30–32]

$$k = k_0 \exp\left\{-\frac{3}{K_p}[(\sigma - \sigma_0) - (p - p_0)]\right\},$$

(5)

where K_p is the pore bulk modulus, $K_p = K\varphi$, and p_0 is the initial gas pressure.

Assumptions are that if $\varepsilon_{xx} = \varepsilon_{yy} = 0$ and $\alpha = 1$, σ_{xx} and σ_{yy} can be expressed as

$$\sigma_{xx} = \sigma_{yy} = \frac{v}{1-v}\sigma_{zz} + \frac{1-2v}{1-v}p + \frac{1-2v}{1-v}K\varepsilon_V.$$

(6)

Change in stress $(\sigma - \sigma_0)$ can be expressed as

$$\sigma - \sigma_0 = \frac{2(1-2v)}{3(1-v)}[(p - p_0) + K(\varepsilon_V - \varepsilon_{V0})].$$

(7)

Substituting formula (7) into formula (5) and combining formulas (2) and (3), we obtained the mathematical model of the permeability change with gas pressure:

$$k = k_0 \exp\left\{\frac{3\Delta p}{\frac{E}{(1-2v)}\phi_0} \cdot \left[\frac{1+v}{1-v} - \frac{2E\varepsilon V_L p_L}{3(1-v)(p_L + p_0)(p + p_L)}\right]\right\}.$$
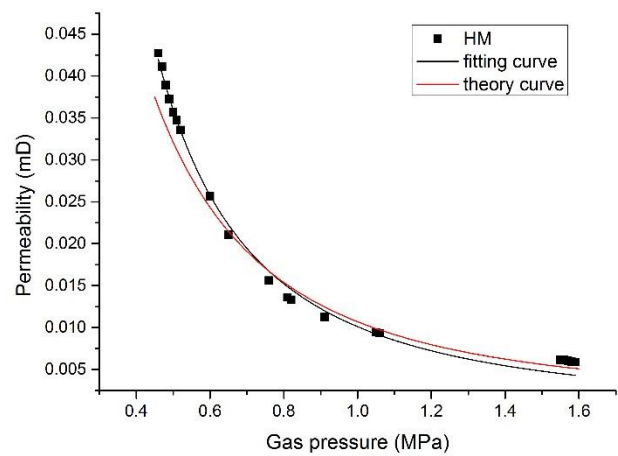
(8)

4.2.2. Experimental verification

By using the basic parameters of the experimental coal samples (Table 3), the theoretical model curves of the permeability of the three coal samples were calculated using formula (8) and compared with the experimental permeability data (Figs. 8-10). The relationship between the permeability value of coal and gas pressure conformed to the power function, and the fitting degree R^2 exceeded 99% (Table 4). The theoretical model and test fitting curves exhibited a high degree of agreement. Coal permeability samples decreased with the increase in gas pressure, and the rate of decrease was fast in the low-pressure section of 0.8 MPa, and slow in the high-pressure section of 0.8~1.5 MPa.

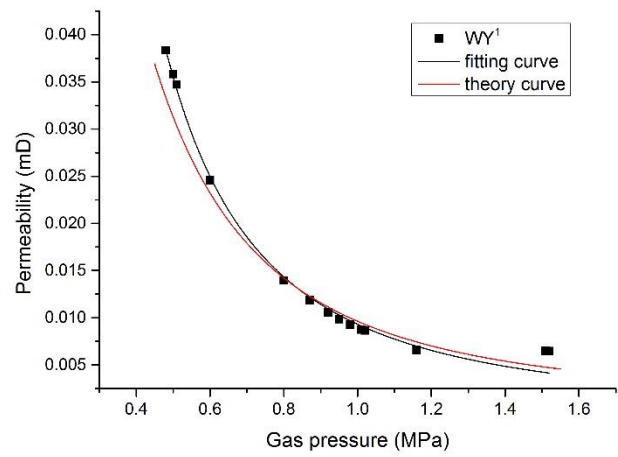**Table 3.** Basic parameters of experimental coal samples.

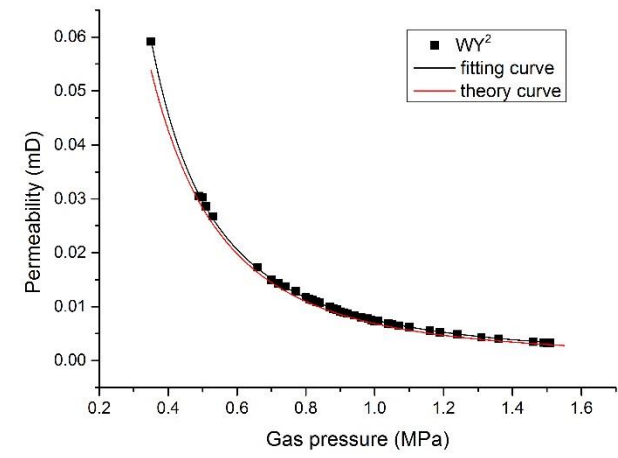| Coal sample	Elastic modulus/GPa	Poisson's ratio	Initial permeability/mD	Initial porosity	Adsorption gas constant/m·t⁻¹	Adsorption gas constant/MPa
HM	1.5	0.35	0.04272	0.09	15.25	4.35
WY[1]	1.7	0.34	0.03834	0.06	24.31	3.89
WY[2]	1.6	0.35	0.03049	0.04	30.58	4.41

Figure 8. Comparison of theoretical model and experimental data of HM.

Figure 9. Comparison of theoretical model and experimental data of WY[1].

Figure 10. Comparison of theoretical model and experimental data of WY[2].

Table 4. Fitting of coal sample permeability and gas pressure.

Coal sample	Fitting equation	Fit R²
HM	$k = 0.01012p^{-1.83137}$	0.99402
WY[1]	$k = 0.00931p^{-1.93214}$	0.99274
WY[2]	$k = 0.00753p^{-1.97026}$	0.99962

As shown in Figures 8 and 10 and Table 5, the theoretical values and experimental data present the same change trend; the difference between the two was mainly concentrated in the low-pressure area below 0.8 MPa, where the theoretical value was lower than the experimental data. The reason for this may be that the theoretical model does not consider the slippage effect, which is more evident in the low-pressure region [33–37]. The maximum absolute error between the theoretical value and experimental data reached 0.00448 mD, and the maximum relative error reached 13.8%. However, overall, the data demonstrate that the basic change trends of the theoretical values and experimental data are consistent. Therefore, according to the basic parameters of the coal samples and the theoretical permeability model, the corresponding permeability under a certain gas pressure can be calculated. The permeability data obtained directly from the experiment truly reflected the change in permeability with gas pressure. However, these experiments only explain the permeability change rule of the experimental coal samples and not coal samples from other places in the coal seam, which is not conducive to engineering applications. Moreover, experimental coal samples are always limited, and testing each location in the coal seam is impossible. The mathematical model of permeability based on desorption-adsorption is critical to understanding the influence mechanism of gas adsorption and gas pressure change on permeability from a microscopic level. This specific expression is obtained using a direct empirical formula and mechanical derivation and has a certain universality, but the key parameters in the mathematical model remain unclear. Therefore, the permeability at different locations in the coal seam can be calculated using this mathematical model.

Table 5. Error analysis between experimental data and theoretical value of permeability.

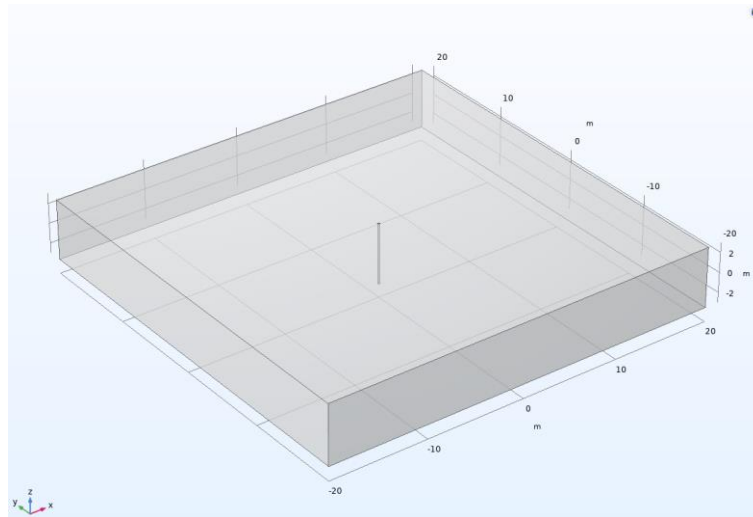| Coal sample	Pressure/MPa	Permeability/mD		Absolute error/mD	Relative error/%
		experimental data	theoretical value		
HM	0.50	0.03570	0.03248	0.00322	9.0
	1.05	0.00944	0.00982	0.00038	4.0
	1.55	0.00617	0.00532	0.00085	13.8
WY[1]	0.50	0.03582	0.03134	0.00448	12.5
	1.01	0.00875	0.00961	0.00086	9.8
	1.51	0.00648	0.00577	0.00071	10.9
WY[2]	0.50	0.03028	0.02830	0.00198	6.5
	1.00	0.00737	0.00687	0.00050	6.7
	1.50	0.00329	0.00299	0.00030	9.1

4.3. Numerical simulation of gas extraction

COMSOL is a finite element analysis software that considers the coupling of multiple physical fields and has achieved good application results in many fields. This study used COMSOL to simulate the coupling of the mechanical field of coal reservoirs and the seepage field of coalbed methane, considering the adsorption/desorption of coalbed methane on the surface of coal seams, diffusion in pores, and the seepage process in fractures. The simulated geometric modeling is a square area, with the length and width set to 40m, the height set according to the thickness of the coal seam at 6 m, and the drilling radius set to 0.1 m with reference to the actual parameters. The established geometric model is shown in Figure 11. The various parameters for the simulation process refer to the onsite

measured values and results in the literature [38-41]. The parameter settings for each module are listed in Table 6.

Table 6. Simulation parameters of gas extraction.

Parameter name	Value [unit]	Describe
E	2650 [MPa]	Elastic modulus of coal
ν	0.35	Poisson's ratio of coal
ϱ	1280 [kg/m³]	Coal seam density
k_0	0.035 [mD]	Initial permeability
φ_0	0.06	Initial porosity
μ	1.00E-5 [Pa·s]	Methane dynamic viscosity
V_L	0.025 [m³/kg]	Langmuir constant
P_L	4 [MPa]	Langmuir pressure
V_M	22.4 [L/mol]	Molar volume of methane under standard conditions
R	8.413510 [J/mol/K]	Gas state constant
T	293 [K]	Sample temperature
M	16 [g/mol]	Gas molecular mass of methane
F_x	15 [MPa]	Confining pressure in X direction
F_y	15 [MPa]	Confining pressure in Y direction
F_z	15 [MPa]	Axial pressure in Z direction
r	0.1 [m]	Borehole radius
p_0	0.5, 0.7, 0.9, 1.1, 1.3, 1.5 [MPa]	Initial pressure
p_b	0.08 [MPa]	Suction negative pressure
t	10 [d]	Adsorption time

Figure 11. Geometric model for numerical simulation of gas extraction.

A linear elastic model was adopted for the solid mechanics module of the simulation. The left, front, and lower interfaces of the model were set as sliding boundaries; thus, the normal upward displacement of the interface was zero. The right, rear, and upper interfaces of the model were set as pressure boundaries, with a pressure of 15 MPa. They simulated the X- and Y-axis stresses of the confining pressure in physical experiments and the Z-axis stress of the axial pressure.

The gas diffusion process in the coal seam pores was simulated using general partial differential equations. The diffusion source term f is represented by the following formula:

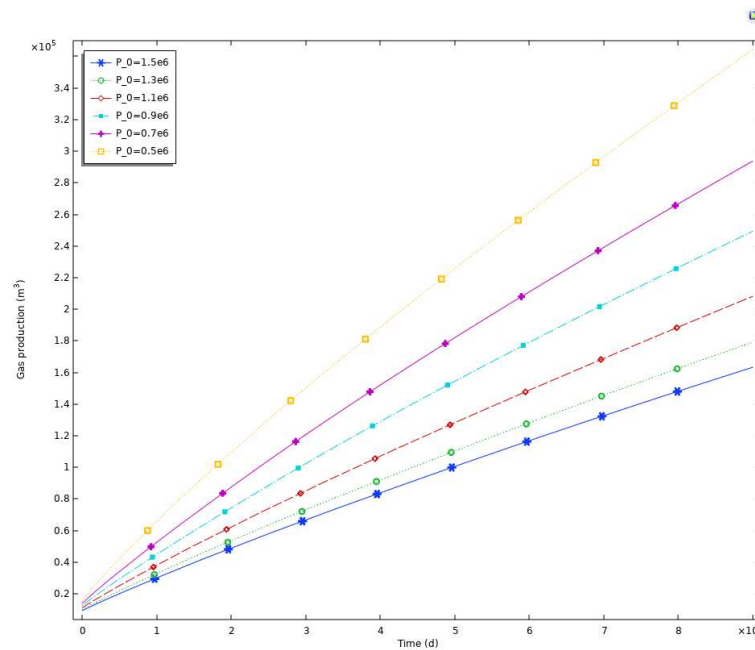$$f = -\frac{V_M(u-p)(u+P_L)^2}{tV_L RTP_L \rho + t\varphi_0 V_M (u+P_L)^2} \tag{9}$$

where u represents the gas pressure in the pore, and p represents the gas pressure in the fracture.

The seepage of coalbed methane in fractures was simulated using Darcy's law. The initial air pressures of the model were 0.5, 0.7, 0.9, 1.1, 1.3, and 1.5 MPa. The negative pressure of the gas extraction hole was set to 0.08 MPa. Permeability k is a function of the gas pressure, and its functional relationship was obtained by fitting the experimental data, set according to the fitting function in Table 4. The expression is as follows:

$$k = 0.00931p^{-1.93214} \tag{10}$$

The numerical simulation results showed (Fig. 12) that with an increase in gas pressure, the efficiency of coal seam gas extraction gradually decreased. When the gas pressure was 0.5 MPa, the daily gas production was approximately 6000 m^3. When the gas pressure increased to 1.5 MPa, the daily gas production decreased to 3000 m^3. In addition, in the low-pressure zone below 0.9 MPa, gas production changed slightly with each increment of 0.2 MPa of gas pressure. However, in the high-pressure zone above 0.9 MPa, gas production changed significantly with each 0.2 MPa of gas pressure. This is also consistent with the law that the permeability of the coal sample changes with the gas pressure obtained from the experiment; that is, the sensitivity coefficient to gas pressure is high in the low-pressure area and low in the high-pressure area.

Figure 12. Comparison of coalbed gas extraction efficiency under different gas pressure.

5. Conclusions

The trend of coal permeability rapidly declined and then slowly declined with an increase in gas pressure, which is in line with the power exponential fitting relationship, and the fitting degree reached more than 99%. In the low-pressure area below 0.8 MPa, the permeability sensitivity coefficient was high. In the high-pressure zone > 0.8 MPa, the permeability sensitivity coefficient was small and tended to be flat. The effect of different coal types on permeability was not obvious. In the same case of coal type, the permeability of the coal sample with the bedding plane parallel to the seepage direction was significantly greater than that with the bedding plane vertical to the seepage direction.

We established a mathematical model considering the relationship between permeability and gas pressure during the adsorption/desorption and seepage processes. The comparison and analysis of the experimental data and theoretical values demonstrated that the mathematical model clearly reflected the trend of coal seam permeability changing with the gas pressure. The maximum relative error between the theoretical value and the experimental data reached 13.8%. However, from the overall data, the basic change trends of the theoretical values and experimental data are consistent. In combination with the test parameters of coal samples, it can be used to predict coal permeability. In the low-pressure section below 0.8 MPa, the theoretical values were generally smaller than the experimental data, which may be related to the slippage effect.

With an increase in gas pressure, coal permeability decreased, and the efficiency of coal seam gas extraction decreased. The gas pressure increased from 0.5 to 1.5 MPa, and the daily gas extraction rate of the coal seam decreased by approximately half. In addition, the reduction rate of gas extraction efficiency in the low-pressure section was greater than that in the high-pressure section.

Author Contributions: Methodology, Jianbao Liu; validation, Bing Li, Jiangang Ren; investigation, Chengtao Yang; writing—original draft preparation, Jianbao Liu; writing—review and editing, Zhimin Song, Shengjie Chen; All authors have read and agreed to the published version of the manuscript.

Institutional Review Board Statement: Not applicable.

Informed Consent Statement: Not applicable.

Data Availability Statement: No applicable.

Conflicts of Interest: The authors declare no conflict of interest.

References

1. Li, N.; Fang, L.; Huang, B.; Chen, P.; Cai, C.; Zhang, Y.; Liu, X.; Li, Z.; Wen, Y.; Qin, Y. Characteristics of Acoustic Emission Waveforms Induced by Hydraulic Fracturing of Coal under True Triaxial Stress in a Laboratory-Scale Experiment. *Minerals* **2022**, 12, 104. https://doi.org/10.3390/min12010104.

2. Song, W.; Yao, J.; Li, Y.; Sun, H.; & Yang, Y. Fractal models for gas slippage factor in porous media considering second-order slip and surface adsorption. *Int. J. Heat. Mass. Tran.* **2018**, *118*, 948-960. https://doi.org/10.1016/j.ijheatmasstransfer.2017.11.072.

3. Liu, S. ; Tang, S. ; & Yin, S. Coalbed methane recovery from multilateral horizontal wells in southern qinshui basin. *Advances in Geo-Energy Research*, **2018**, 2(1), 34-42.

4. Ye, D. ; Liu, G. ; Gao, F.;, Xu, R. ; & Yue, F. A multi-field coupling model of gas flow in fractured coal seam. *Advances in Geo-Energy Research*, **2021**, 5(1), 104-118.

5. Tian, Y.; Yu, X.; Li, J.; Yin, X.; Neeves, K. B.; & Wu, Y. S. Scaling law for slip flow of gases in nanoporous media from nanofluidics, rocks, and pore-scale simulations. *Fuel* **2018**, *1*, 1-23. https://doi.org/10.1016/j.fuel.2018.09.036.

6. Li, W.; Jiang, B.; Zhu, Y. Impact of tectonic deformation on coal methane adsorption capacity. *Adsorpt. Sci. & Techno.* **2019**, 37, 698 -708.

7. Cai, J.; Wei, W.; E. I.; Hu, X.; Liu, R.; & Wang, J. Fractal characterization of dynamic fracture network extension in porous media. *Fractals* **2017**, *25*, 1750023. https://doi.org/10.1142/S0218348X17500232.

8. Chen, Z.; Li, G.; Wang, Y.; Li, Z.; Chi, M.; Zhang, H.; Tian, Q.; Wang, J. An Experimental Investigation of the Gas Permeability of Tectonic Coal Mineral under Triaxial Loading Conditions. *Minerals* **2022**, 12, 70. https://doi.org/10.3390/min12010070.

9. Liu, C.; Yin, G.; Li, M.; Shang, D.; Deng, B.; & Song, Z. Deformation and permeability evolution of coals considering the effect of beddings. *Int. J. Rock. Mech. Min.* **2019**, *117*, 49-62. https://doi.org/10.1016/j.ijrmms.2019.03.016.

10. Liu, J.; Song, Z.; Yang, C.; Li, B.; Ren, J.; & Xiao, M. True triaxial experimental study on the influence of axial pressure on coal permeability. *Front. Earth. Sc-switz.* **2022**, *10*, 1024483. https://doi.org/10.3389/feart.2022.1024483.

11. Xiong, J.; Liu, X.; & Liang, L. Application of adsorption potential theory to methane adsorption on organic-rich shales at above critical temperature. *Environ. Earth. Sci.* **2018**, *77*, 1-18. https://doi.org/10.1007/s12665-018-7247-3.

12. Liu, J.; Gao, J.; Zhang, X.; Jia, G.; & Wang, D. Experimental study of the seepage characteristics of loaded coal under true traxial conditions. *Rock. Mech. Rock. Eng.* **2019**, *52*, 2815-2833. https://doi.org/10.1007/s00603-018-1720-x.

13. Liu, J.; Song, Z.; Li, B.; Ren, J.; Chen, F.; & Xiao, M. Experimental Study on the Microstructure of Coal with Different Particle Sizes. *Energies* **2022**, *15*, 4043. https://doi.org/10.3390/en15114043.

14. Liu, Y.; Yin, G.; Li, M.; Zhang, D.; Deng, B.; Liu, C.; & Lu, J. Anisotropic mechanical properties and the permeability evolution of cubic coal under true triaxial stress paths. *Rock. Mech. Rock. Eng.* **2019**, *52*, 2505-2521. https://doi.org/10.1007/s00603-019-01748-1.

15. Xie, J.; Gao, M.; Yu, B.; Zhang, R.; & Jin, W. Coal permeability model on the effect of gas extraction within effective influence zone. *Geomech. Geophys. Geo.* **2015**, *1*, 15-27. https://doi.org/10.1007/s40948-015-0002-2.

16. Yu, B.; Liu, C.; Zhang, D.; Zhao, H.; Li, M.; Liu, Y.; ... & Li, H. Experimental study on the anisotropy of the effective stress coefficient of sandstone under true triaxial stress. *J. Nat. Gas. Sci. Eng.* **2020**, *84*, 103651. https://doi.org/10.1016/j.jngse.2020.103651.

17. Liu, Y.; Li, M.; Yin, G.; Zhang, D.; & Deng, B. Permeability evolution of anthracite coal considering true triaxial stress conditions and structural anisotropy. *J. Nat. Gas. Sci. Eng.* **2018**, *52*, 492-506. https://doi.org/10.1016/j.jngse.2018.02.014.

18. Letham, E. A.; & Bustin, R. M. The impact of gas slippage on permeability effective stress laws: implications for predicting permeability of fine-grained lithologies. *Int. J. Coal. Geol.* **2016**, *167*, 93-102. https://doi.org/10.1016/j.coal.2016.09.015.

19. Lu, J.; Yin, G.; Deng, B.; Zhang, W.; Li, M.; Chai, X.; ... & Liu, Y. Permeability characteristics of layered composite coal-rock under true triaxial stress conditions. *J. Nat. Gas. Sci. Eng.* **2019**, *66*, 60-76. https://doi.org/10.1016/j.jngse.2019.03.023.

20. Zimmerman, R. W. Coupling in poroelasticity and thermoelasticity. *Int. J. Rock. Mech. Min.* **2000**, *37*, 79-87. https://doi.org/10.1016/S1365-1609(99)00094-5.

21. Neuzil, C. E. Hydromechanical coupling in geologic processes. *Hydrogeol. J.* **2003**, *11*, 41-83. https://doi.org/10.1007/s10040-002-0230-8.

22. Palciauskas, V. V.; & Domenico, P. A. Characterization of drained and undrained response of thermally loaded repository rocks. *Water. Resour. Res.* **1982**, *18*, 281-290. https://doi.org/10.1029/wr018i002p00281.

23. Cao, P.; Liu, J.; & Leong, Y. K. General gas permeability model for porous media: bridging the gaps between conventional and unconventional natural gas reservoirs. *Energ. fuel.* **2016**, *30*, 5492-5505. https://doi.org/10.1021/acs.energyfuels.6b00683.

24. Si, L.; Li, Z.; & Yang, Y. Coal permeability evolution with the interaction between nanopore and fracture: Its application in coal mine gas drainage for Qingdong coal mine in Huaibei coalfield, China. *J. Nat. Gas. Sci. Eng.* **2018**, *56*, 523-535. https://doi.org/10.1016/j.jngse.2018.06.032.

25. Yu, P.; Liu, Y.; Wang, J.; Kong, C.; Gu, W.; Xue, L.; ... & Jiang, L. A new fracture permeability model: Influence of surrounding rocks and matrix pressure. *J. Pet. Sci. Eng.* **2020**, *193*, 107320. https://doi.org/10.1016/j.petrol.2020.107320.

26. Duan, M.; Jiang, C.; Gan, Q.; Li, M.; Peng, K.; & Zhang, W. Experimental investigation on the permeability, acoustic emission and energy dissipation of coal under tiered cyclic unloading. *J. Nat. Gas. Sci. Eng.* **2020**, *73*, 103054. https://doi.org/10.1016/j.jngse.2019.103054.

27. Duan, M.; Jiang, C.; Gan, Q.; Zhao, H.; Yang, Y.; & Li, Z. Study on permeability anisotropy of bedded coal under true triaxial stress and its application. *Transport. Porous. Med.* **2020**, *131*, 1007-1035. https://doi.org/10.1016/j.jngse.2020.103651.

28. Duan, M.; Jiang, C.; Xing, H.; Zhang, D.; Peng, K.; & Zhang, W. Study on damage of coal based on permeability and load-unload response ratio under tiered cyclic loading. *Arab. J. Geosci.* **2020**, *13*, 1-11. https://doi.org/10.1007/s12517-020-5249-4.

29. Zhu, W. C.; Wei, C. H.; Liu, J.; Qu, H. Y.; & Elsworth, D. A model of coal–gas interaction under variable temperatures. *Int. J. Coal. Geol.* **2011**, *86*, 213-221. https://doi.org/10.1016/j.coal.2011.01.011.

30. Liu, Q.; Li, Z.; Wang, E.; Niu, Y.; & Kong, X. A dual-permeability model for coal under triaxial boundary conditions. *J. Nat. Gas. Sci. Eng.* **2020**, *82*, 103524. https://doi.org/10.1016/j.jngse.2020.103524.

31. Gao, Q.; Liu, J.; Huang, Y.; Li, W.; Shi, R.; Leong, Y. K.; & Elsworth, D. A critical review of coal permeability models. *Fuel* **2022**, *326*, 125124. https://doi.org/10.1016/j.petrol.2020.108283.

32. Liu, T.; Lin, B.; & Yang, W. Impact of matrix–fracture interactions on coal permeability: model development and analysis. *Fuel* **2017**, *207*, 522-532. https://doi.org/10.1016/j.fuel.2017.06.125.

33. Li, B.; Ren, J.; Liu, J.; Liu, G.; Lv, R.; & Song, Z. Diffusion and Migration Law of Gaseous Methane in Coals of Different Metamorphic Degrees. *Int. J. Heat. Technol.* **2019**, *37*, 1019-1030. https://doi.org/10.18280/ijht.370411.

34. Liu, J.; Song, Z.; Li, B.; Ren, J.; Chen, F.; Xiao, M.; & Yang, C. Study on the Destructive Effect of Small Faults on Coal Pore Structure. *Geofluids* **2022**, *2022*, *2124853*. https://doi.org/10.1155/2022/2124853.

35. Ren, J.; Song, Z.; Li, B.; Liu, J.; Lv, R.; & Liu, G. Structure feature and evolution mechanism of pores in different metamorphism and deformation coals. *Fuel* **2021**, *283*, 119292. https://doi.org/10.1016/j.fuel.2020.119292.

36. Zhou, Y.; Li, Z.; Yang, Y.; Zhang, L.; Si, L.; Kong, B.; & Li, J. Evolution of coal permeability with cleat deformation and variable Klinkenberg effect. *Transport. Porous. Med.* **2016**, *115*, 153-167. https://doi.org/10.1016/j.jngse.2016.02.049.

37. Zhu, W.; Liu, L.; Liu, J.; Wei, C.; & Peng, Y. Impact of gas adsorption-induced coal damage on the evolution of coal permeability. *Int. J. Rock. Mech. Min.* **2018**, *101*, 89-97. https://doi.org/10.1016/j.ijrmms.2017.11.007.

38. Wang, C.; Zhang, J.; Zang, Y.; Zhong, R.; Wang, J.; Wu, Y.; ... & Chen, Z. Time-dependent coal permeability: Impact of gas transport from coal cleats to matrices. *J. Nat. Gas. Sci. Eng.* **2021**, *88*, 103806. https://doi.org/10.1016/j.jngse.2021.103806.

39. Cai, J.; Wood, D. A.; Hajibeygi, H.; & Iglauer, S. Multiscale and multiphysics influences on fluids in unconventional reservoirs: Modeling and simulation. *Ager* **2022**, *6*, 91-94. https://doi.org/10.46690/ager.2022.02.01.

40. Zimmerman, R. W.; Somerton, W. H.; & King, M. S. Compressibility of porous rocks. *J. Geophys. Res-sol.* Ea. **1986**, *91*, 12765-12777. https://doi.org/10.1029/JB091iB12p12765.

41. Liu, G.; Liu, J.; Liu, L.; Ye, D.; & Gao, F. A fractal approach to fully-couple coal deformation and gas flow. *Fuel* **2019**, *240*, 219-236. https://doi.org/10.1016/j.fuel.2018.11.140.